Composites: Part A 84 (2016) 266–280

Contents lists available at ScienceDirect

Composites: Part A

journal homepage: www.elsevier.com/locate/compositesa

Mechanical properties of 3D printed interpenetrating phase composites with novel architectured 3D solid-sheet reinforcements

Ahmed S. Dalaq, Diab W. Abueidda, Rashid K. Abu Al-Rub *

Institute Center for Energy, Mechanical and Materials Engineering Department, Masdar Institute of Science and Technology, Abu Dhabi, United Arab Emirates

ARTICLE INFO

Article history:
Received 10 November 2015
Received in revised form 27 January 2016
Accepted 7 February 2016
Available online 13 February 2016

Keywords:
Interpenetrating phase composites
D. Mechanical testing
B. Mechanical properties
A. 3-Dimensional reinforcement
E. 3D printing

ABSTRACT

Interpenetrating phase composites (IPCs) are novel types of multifunctional composite materials. This work focuses on investigating experimentally and computationally the mechanical behavior of novel types of three-dimensional (3D) architectured two-phase IPCs. The current IPCs are architectured using several morphologies of the fascinating and mathematically-known triply periodic minimal surfaces (TPMS) that promote several multifunctional attributes. Specifically, the second hard reinforcing phase takes the architecture of one of the 3D non-intersecting and continuous TPMS-based solid sheets. The mechanical response of the 3D printed polymer-based IPCs is measured under uniaxial compression where the effect of varying the second-phase architecture and volume fraction is explored. Anisotropy induced by the 3D printing is also investigated. 3D finite element analysis has been performed and validated for predicting elastic properties of the various types of TPMS-based IPCs. The most effective TPMS architecture in enhancing the mechanical properties and damage-tolerance has been identified.

1. Introduction

Nature found its way to achieve optimized and multifunctional structures and materials. An example of these structures is the triply periodic minimal surfaces/shells (TPMS) (see Fig. 1) that, mathematically, are created by enforcing the local area minimization principle [e.g., 1,2–4], which creates surfaces that divide 3D space into two non-self-intersecting bi-continuous phases. These TPMS structures (or architectures) occur in various biological systems such as: beetle shells, butterfly wings, and weevils [e.g., 5,6]. Inspired by these natural structures, new man-made composites fabricated from a wide range of solid constituents are desirable for a wide range of applications based on the fact that each architecture embodies a reinforcement that interacts uniquely with a matrix regardless of their constituents (i.e., we focus on the architecture). Such 3D TPMS interconnected geometries can be used as second-phase material reinforcements [7–13] in order to produce interpenetrating phase composites (IPC) of various architectures where most desirable properties of both solid constituents (base materials) are combined. IPCs are a novel type of composites in which each solid phase is not-isolated but forms an interconnected solid networks such that if one of the phases is removed the remaining phase(s) give a stand-alone open-celled foam [e.g., 14,15–17]. By local area minimization in TPMS (i.e., meaning the smallest surface area within a given boundary) the surface tension is minimized along with surface energy and thereby minimizes the residual stress [18], which is desirable for IPCs. Also, TPMS topology is known for multifunctionality [12,19,20], mathematical precision (accurate mathematical representation) [19], optimized topology for mechanical applications [21], where it possess geometrical, thermal and electrical extremals [20]. There are many architectures for TPMS; however, in this paper, we investigate the mechanical properties of IPCs created using one of the most common TPMS architectures shown in Fig. 1(c)–(i) and used as a 3D solid sheet/shell reinforcement.

Initially, the TPMS were studied in the realm of mathematics, in fact they were primarily perceived by mathematician through optimization [1,2]. However, this optimization happened to be a property that nature has already formed in the microstructures of many biological systems, as stated earlier. For that reason, the most extensive work on TPMS by far was made in the field of biomaterials [e.g., 19,22,23]. The TPMS can be idealized as a skeleton (i.e., a truss-like structure) which is a scheme recently used in [24] to model Gyroid (Fig. 1(h)) as a lattice-foam for which elastic and plastic properties are computed. Besides the practicality of this approach, Maldovan et al. [25] argued that such idealization does not capture the geometrical intricacy and curvatures of TPMS architectures and hence produces less accurate properties. On the

* Corresponding author. Tel.: +971 2810 9162; fax: +971 2810 9901.
E-mail addresses: rabualrub@masdar.ac.ae, rashedkamel@yahoo.com (R.K. Abu Al-Rub).

http://dx.doi.org/10.1016/j.compositesa.2016.02.009
1359-835X/

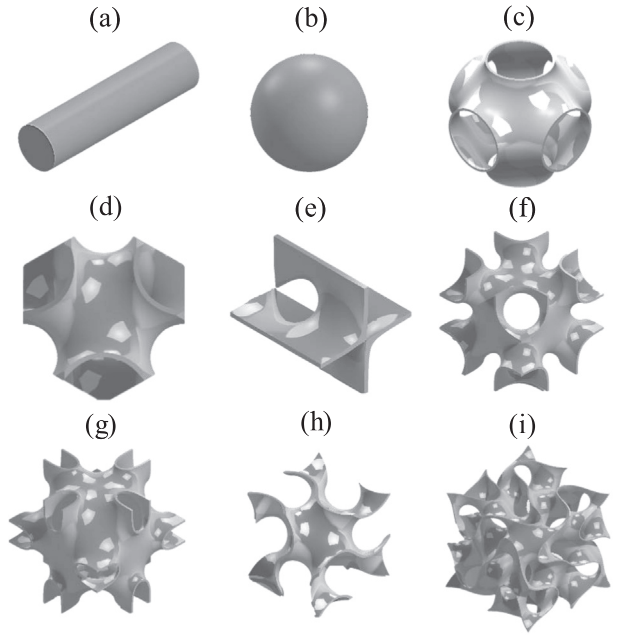

Fig. 1. (a) and (b) are common reinforcement geometry; (a) discontinuous periodic-fibers and (b) periodic-particles, whereas (c)-(l) are the new investigated 3D architectures referred to as TPMS (triply periodic minimal surfaces or sheets); (c) Schwarz P (Primitive), $g = 3$, (d) Schwarz D (Diamond-rhombic), $g = 3$, (e) Schwarz CLP (CLP) $g = 3$, (f) Schoen I-WP (IWP), $g = 7$, (g) Neovius C(P) (Neovius), $g = 9$, (h) Schoen G (Gyroid), $g = 3$, and (i) Fischer-Koch S (S).

other hand, TPMS-based IPCs or porous media of high solid volume fractions (greater than 50%), which utilize the TPMS topology from only one surface that is in contact with the second-phase material, has been the focus of few studies. For example, Wang et al. [13] used this approach to create and 3D print IPCs with Schwarz Primitive solid networks (not solid sheets which is the focus of the current paper) at high volume fractions (30–60%), where its mechanical properties are assessed using uniaxial compressing testing and hyperelastic–plastic computational modeling. Kadkhodapour et al. [26] have conducted experimental and computational evaluation of several TPMS-based solid networks porous media (not a composite). However, creating the TPMS as solid sheets or shells (as opposed to solid networks) utilizing their topologies from both sides of their surfaces and with lower solid volume fractions ($\leqslant 30\%$) is a novel idea proposed in [7,19]. Therefore, here in this work, we employ the TPMS as 3D reinforcements by converting the TPMS surfaces to very thin solid sheets (see Fig. 1(c)–(i)) without any parametric approximations or strut/skeleton idealizations. We have previously implemented this approach and computationally approximated the thermal and electrical properties of the TPMS-IPCs [7–10]. For example, in [7,10] it is demonstrated that TPMS-IPCs can produce significant enhancement in thermal/-electrical conductivity in comparison to traditional composites, whereas in [8] carbon nanostructured-epoxy TPMS reinforcements have been incorporated into 3D printing materials to make them electrical conductive. In addition, micromechanical models of each TPMS were used to evaluate and compare the reduced coefficient of thermal expansion of each TPMS-IPC [9].

In this study, the overall stress–strain behavior of seven various types of 3D printed TPMS-based IPCs are evaluated experimentally (see Fig. 2). Firstly, elastic and inelastic behavior of base materials (i.e., the matrix and reinforcement materials) is assessed. Secondly, elastic properties of the seven TPMS-IPCs are evaluated and compared to finite element prediction results. Thirdly, the TPMS-IPCs' compressive inelastic behavior including the evaluation of their effective ultimate strength, toughness, and strain at failure are reported and discussed. Fourthly, evaluation of the degree of improvement induced by reinforcing the matrix with TPMS sheets is performed. Accordingly, a more extensive experimental and computational analysis is conducted for the most effective TPMS.

2. Methodology

2.1. Creating TPMS-IPCs

We created 3D computer aided design (CAD) models for the TPMS and their corresponding complementary parts (the enclosing matrix) using a series of visualization software. Fig. 3 schematically shows how this is done for the Primitive TPMS-based IPC (P-IPC). The mathematical representation of each TPMS was retrieved from [27,28] using the *surface evolver* software. Each STL (voxel based) file was thickened by offsetting each voxel to a value determined by the desired TPMS volume fraction. Then, the thickened TPMS is subtracted from a unit-cell cube using *SolidWorks*, thereby creating the complementary matrix part. Both parts, the complementary part and the reinforcement, are converted from CAD to sterolithography (STL) format, transferred to object studio software and printed using object Connex 260 3D printer [29] (see Fig. 2).

The base materials of the 3D printer are vendor based, and we have chosen a contrasting pair of materials, namely, Tango-Plus (FLX930), and Vero-Plus (RGD875) [29]. These materials belong to "PolyJet" materials a trade mark of Stratasys [29]. All tested specimens were manufactured by Object260 Connex 3D printer (see Fig. 4) with layer thickness deposition of 16 μm, and accuracy of 20–85 μm. Object Studio Software was used to transform TPMS-IPC CAD models to STL files, and as an interface to connect and transfer data to the 3D printer. Three cubic specimens ($30 \times 30 \times 30$ mm) of Tango-plus and Vero-plus were printed (see Fig. 5) and mechanically tested.

2.2. Mechanical testing procedure

Each of the printed specimens was tested under displacement control compression or tension using Instrone 5980 series with a 5 kN load cell. We examined the 3D printing base materials response under various printing directions, see Figs. 5 and 6. For each data point, three specimens have been tested and the standard deviation was reported. Note that the stress–strain curves exhibit a nonlinear behavior at low strains. This is attributed to misalignments and surface roughness; therefore, the specimens were slightly pre-compressed prior to loading in order to reduce the effect of misalignment.

Uniaxial compression testing was done on cubic samples (see Figs. 2, 5 and 7), whereas the ASTM D638-10 standard for uniaxial tension was followed to further prove that printing direction affects the mechanical behavior of the printed materials (see Fig. 6). ASTM standard uniaxial tensile specimens (Fig. 6) are printed in only two directions (i.e., X_2 and X_3) as it was difficult to print such specimens in the X_1-direction; see Figs. 4 and 6. Each tensile test is repeated for three replicates. The tensile specimens are tested under displacement controlled until failure. Using the data from uniaxial tension and compression tests, the behavior of both printing materials (i.e., Tango-Plus and Vero-Plus) under tension and compression are compared.

In order to evaluate the mechanical properties of the base materials (i.e., Vero-Plus and Tango-Plus) in compression, we have tested three Tango-Plus and Vero-Plus cubic specimens till failure for each direction. The Young's modulus, ultimate strength, strain at failure, and toughness (area under the stress–strain diagram